Send Orders for Reprints to reprints@benthamscience.net

Current Drug Metabolism, 2020, *22*, 1-0

RESEARCH ARTICLE

A Novel Nanoformulation of Ellagic Acid is Promising in Restoring Oxidative Homeostasis in Rat Brains with Alzheimer's Disease

Steve Harakeh[1,2,*], Mohamad H. Qari[3], Wafaa S. Ramadan[4,5], Soad K. Al Jaouni[2,6], Mohammed S. Almuhayawi[7], Turki Al Amri[8], Ghulam Md Ashraf[9,10], Dhruba J Bharali[11] and Shaker A Mousa[1,2,*]

[1]Special Infectious Agents Unit, King Fahd Medical Research Center, King Abdulaziz University (KAU); [2]Yousef Abdul Latif Jameel Scientific Chair of Prophetic Medicine Application, Faculty of Medicine, KAU; [3]Department of Hematology, King Abdulaziz University (KAU), Jeddah, Saudi Arabia; [4]Department of Anatomy, Faculty of Medicine, KAU, Saudi Arabia; [5]Department of Anatomy, Ain Shams University, Cairo, Egypt; [6]Department of Hematology/ Pediatric Oncology, King Abdulaziz University Hospital (KAUH), Faculty of Medicine (FM), KAU; [7]Department of Medical Microbiology/Parasitology and Molecular Microbiology Laboratory, KAUH, KAU; [8]Family and Community Medicine Department, Faculty of Medicine in Rabigh, King Abdulaziz University, Jeddah, Saudi Arabia; [9]King Fahd Medical Research Center, King Abdulaziz University, Jeddah, Saudi Arabia; [10]Department of Medical Laboratory Technology, Faculty of Applied Medical Sciences, King Abdulaziz University, Jeddah, Saudi Arabia; [11]Albany Nutraceuticals, Rensselaer, NY, 12144, USA; [12]Pharmaceutical Research Institute, Albany College of Pharmacy and Health Sciences, Rensselaer, NY, USA

ARTICLE HISTORY

Received: April 16, 2020
Revised: October 08, 2020
Accepted: October 21, 2020

DOI:
10.2174/1389200221666201216170851

Abstract: ***Background*:** Aluminum toxicity induces neurodegenerative changes in the brain and results in Alzheimer's disease (AD).

***Objective*:** Here, the aim was to evaluate the antioxidant therapeutic effects of ellagic acid (EA) and EA-loaded nanoparticles (EA-NP) in an aluminum chloride-induced AD rat model.

***Methods*:** The nanoparticles' loading of EA was 0.84/1 w/w. The *in vitro* release kinetics of EA from EA-NP in fetal bovine serum showed 60% release in the first 1-5 hours, followed by sustained release at 60-70% over 6-24 hours. Six groups were implemented; group 1 served as the control, group 2 received EA, group 3 received EA-NP, group 4 was the AD rat model administered $AlCl_3$ (50 mg/kg) for 4 weeks, groups 5 (AD+EA) and 6 (AD+EA-NP) were treated with EA and EA-NP, respectively, for 2 weeks after $AlCl_3$ was stopped. The neurotoxicity in the rat brain was examined by measuring the brain antioxidant biomarkers catalase, glutathione, and total antioxidant activity and lipid peroxidation (thiobarbituric acid, TBA). Histopathological studies using hematoxylin and eosin, cresyl violet, silver stains, and the novel object recognition test were examined.

***Results*:** Data revealed significant increase of antioxidant biomarkers and decreased TBA in the EA-NP group. The pathological hallmarks of AD-vacuolation of the neurons, chromatolysis, neurofibrillary tangles, and the senile plaques in brains of the AD rat model were decreased and restoration of Nissl granules was noted. The calculated discrimination index in the behavioral test increased more in cases treated with EA-NP.

***Conclusion*:** The treatment of AD with EA-NP was more effective than EA in alleviating the oxidative neurotoxic effects on AD rat brains.

Keywords: Alzheimer's disease, aluminum, oxidative stress, antioxidant biomarkers, ellagic acid, nanoformulation, nano-Ellagic acid, neuroprotection.

1. INTRODUCTION

Alzheimer's disease (AD) is a severe neurodegenerative disorder in the elderly [1] manifested by cognitive and memory deterioration, behavioral disturbances, and neuropsychiatric symptoms [2]. Peroxidation, a hallmark of oxidative tissue injury, has been found to be elevated in AD brain [3].

Although minimal intake of 1 mg/kg body weight/day of aluminum as declared by the World Health Organization is not hazardous (WHO, 2001), exposure to large doses over time is a toxic hazard. In addition to being a constituent of antacids and food additives, the use of aluminum food wrapping sheets allows easy access of aluminum into the body [4]. The neurotoxicity of aluminum in animal studies is documented. Aluminum's toxicity was attributed to the potentiation of oxidative damage activity caused by Fe^{2+} and Fe^{3+} ions, considered to be one of the causes of neurodegenerative diseases like AD [4].

In the course of an ongoing search for bioactive plant-derived natural products in treating neurodegenerative diseases, many herbs and plant extracts have been examined. In the present work, ellagic acid (EA) was investigated as an antioxidant therapeutic for AD. EA is a non-flavonoid polyphenol and is present in fruits, food, and beverages. It has been proven to have antioxidant, anti-inflammatory, antiproliferative, antidiabetic, and cardioprotective properties [5-9]. It has been documented that ellagic acid is not well absorbed and is quickly removed from the body [10]. This has increased the interest of pharmaceutical industries in nanotechno-

* Address correspondence to these authors at the Special Infectious Agents Unit, King Fahd Medical Research Center, King Abdulaziz University (KAU);
Tel: 00966559392266; Fax: 0096626952076; E-mails: sharakeh@gmail.com, shaker.mousa@acphs.edu

1389-2002/20 $65.00+.00

logical advances in order to enhance the effectiveness and selectivity of active components and improve drug delivery systems [11].

The aim of the present work was to assess the antioxidant activities of EA and EA-loaded nanoparticles on the brains of rats in an aluminum chloride ($AlCl_3$) induced AD model and identify the effective form in the restoration of oxidative homeostasis. It is well known that because free radicals' generation exceeds the body's ability to neutralize them, oxidative stress occurs. In the present work, the total antioxidant capacity (TAC) and two antioxidants [glutathione (GSH) and catalase] were assessed. In addition, lipid peroxidation was evaluated by measuring thiobarbituric acid reactive substances (TBARS).

2. MATERIALS AND METHODS

2.1. Materials

EA, $AlCl_3$ and cholesterol were obtained from Sigma Aldrich (St. Louis, MO, USA). PLGA Nanoparticles (PLGA-NP), Polyvinyl alcohol were bought from Evonik (Waterford, NY USA). Tween 80 and Mannitol from Sigma Aldrich were used as stabilizers and cryoprotectant, respectively, for the nanoparticles. Other common reagents were obtained from Sigma Aldrich.

2.2. Animals

Sixty male adult Wistar albino rats, ranging in weight from 200-250 g each, were obtained from King Abdulaziz University (KAU), Jeddah, Saudi Arabia. The animals were maintained in wire-meshed cages at 22 ± 2°C, 55% humidity, and light/dark of 12/12 hours ratio. Purina chow diet and ad libitum drinking water were offered.

2.3. Nanoparticle Synthesis

Poly (lactic-co-glycolic acid) nanoparticles (PLGA-NPs) encapsulating EA were obtained as previously described [12]. PLGA polymer stock solution was achieved by thoroughly mixing 80 mg/ml in dichloromethane. A 10 mg/ml stock solution of EA (33 µM of EA) was used. Five hundred µl of each stock solution was mixed together by vortexing. In order to obtain primary emulsion, 1 ml of this solution was added to 200 µl of PBS by intermittent sonication (2-3 times, 30 sec each time) to produce an emulsion, which was emulsified after sonication in 2 ml of 1% w/v polyvinyl alcohol (PVA) solution for 30 seconds. 40 ml of 1.0% PVA solution was added to the emulsion and mixed by magnetic attiring for 30 minutes. A rotatory evaporator was used to evaporate dichloromethane at 37 °C. A 10-12 KD cutoff dialysis membrane was then used in order to dialyze the whole solution for 24 hours using distilled water to get rid of any free non-encapsulated EA present. The whole solution was lyophilized and suspended to be used in subsequent experiments in the presence of 4% mannitol.

2.3.1. Dynamic Light Scattering for Nanoparticles Size Management

Dynamic light scattering (DLS) utilizing a Malvern zeta sizer (Malvern Instrumentation Co, Malvern, PA) was employed to determine the EA-NPs size distribution in aqueous dispersion. After redispersion of the lyophilized powder in deionized water, DLS was used directly to measure the size distribution of 1 ml of NP solution after mixing it in 3 ml of a 4-sided clear plastic cuvette.

2.3.2. Entrapment Efficiency

EA encapsulated amount present in the NPs was assayed by dispersing the NPs. Then, the compound was measured using UV-VIS spectroscopy and HPLC.

The entrapment efficiency was calculated, as shown below:

Entrapment efficiency (loading) = $([Drug]_f)^* / ([Drug]_t)^{**} \times 100$

* $[Drug]_f$ is the EA in the NPs and ** $[Drug]_t$ is the theoretical level of the product

2.4. Characterization of EA PLGA Nanoformulation

Particle size and loading efficiency of EA in the nanoparticles were determined using DLS for the average size and UV-VIS spectroscopy and HPLC for EA loading into the nanoformulation.

2.5. *In vitro* Release Kinetics of EA from EA-NP

in vitro release of EA in fetal bovine serum (FBS) versus phosphate buffered saline (PBS) was carried out with EA loaded PLGA nanoparticle formulations using the dialysis bag diffusion method [13]. Drug loaded nanoparticles (5 ml) were dispersed into the dialysis bag, and the dialysis bag was then kept in a beaker containing 100 ml of pH 7.4 phosphate buffer. The beaker was placed over a magnetic stirrer and the temperature of the assembly was maintained at 37 ± 1 °C throughout the experiment. During the experiment, rpm was maintained at 100 rpm. Samples (2 ml) were withdrawn at a definite time interval (0.5, 1, 1.5, 2, 3, 4, 6, 9, 12 and 24 hours) and replaced with equal amounts of fresh pH 7.4 phosphate buffer. After suitable dilutions, the samples were analyzed using UV-Visible spectrophotometer. To analyze the *in vitro* drug release data, various kinetic models were used to describe the release kinetics.

2.6. Animal Study Design

Six groups of rats were used, 10 rats in each. The dose of EA was calculated based on the nanoparticles' loading of EA (loading = 0.84%w/w) per kg of rat and the best entrapment efficacy as detected with UV-Vis spectra. The calculated oral dose was 1.19 mg/kg body weight.

Group I (control): Rats in this group acted as negative control and received the same amount of water and food as all other groups. Group II (EA): Rats received EA dissolved in DMSO for 14 days. Group III (EA-NP): Rats received EA-NP for 2 weeks. Group IV (AD): Rats received aluminum chloride ($AlCl_3$, 50 mg/kg) dissolved in water for 4 successive weeks daily [14]. Group V (AD+EA-NP): Rats received EA-NP formulation. Group VI (AD+EA): Rats received EA. In groups V and VI, treatment continued for 2 weeks after $AlCl_3$ administration was stopped. Rats received all medications by oral administration Table **1**.

Table 1. List of animal groups, treatment received and the duration.

Group	Treatment	Treatment Length
Control	-	-
EA	EA in DMSO	14 days
EA-SLNP	EA in nanoparticles	14 days
AD	$AlCl_3$ (50 mg/kg) in water	4 weeks
AD+EA	EA given after $AlCl_3$ was stopped	14days
AD+EA-SLNP	EA -SLNP given after $AlCl_3$ was stopped	14 days

2.7. Behavioral Tests

Animals were subjected to the novel object recognition test before and after induction of AD (administered $AlCl_3$ (50 mg/kg) and after treatment.

2.8. Recognition of Novel Objects

This test evaluated the potential of the rat to identify a novel object in the arena. It consists of three stages: habituation, familiarization, and test. In the habituation stage, each animal explored the empty arena for 5 minutes. Then the rat was put back in its original cage. During the familiarization stage, two identical objects were placed in an open-field arena, and a single rat was allowed to explore them for 5 minutes, then returned to its holding cage. During the test stage, the rat returned to the open-field arena with two objects-one was the same object used before and the other was a novel, new object. A normal rat should increase its presence at the novel object. The time required to explore the novel object was measured (the discrimination index = DI) with Etho Vision video tracking software, version xt8 [15].

The total exploration time in both sessions was calculated according to DI [16].

$$DI = \frac{\text{Exploration of novel object (NO)} - \text{Exploration of familiar object (FO)}}{(NO + FO)}$$

2.9. Brain Tissue Sampling

The rats were sacrificed by decapitation at the end of the experiment (6 weeks) after fasting for 12 h. immediately after that, each rat brain was harvested and dissected and left in isotonic saline to be thoroughly washed, then weighed after drying. The brain was then split into two parts. One part was used for the preparation of the brain homogenate and the other portion was used for histopathological examination.

2.10. Preparation of Brain Homogenate

Homogenization of brain tissue was done 10 times in ice- cold 0.1 M phosphate buffer saline. The resulting supernatant was obtained by centrifugation for 15 mins at 10,000 g of the homogenate and aliquots were used for biochemical testing [17].

2.11. Biomarkers for Antioxidant Activity

2.11.1. Catalase activity measurement

Catalase activity was determined by UV spectrophotometry at 240 nm expressed as % activity following [18]. This is based on the fact that the rate of catalase activity corresponds to the rate of dissociation of hydrogen peroxide.

2.11.2. Estimation of GSH

GSH concentration in the brain tissue was determined as described elsewhere [19], based on the reaction of 5,5′ dithio-bis-(2-nitrobenzoic acid (DTNB)) with the presence of products having the sulfhydryl groups. Glutathione concentration was presented as µmol per mg protein.

2.11.3. Estimation of Total Antioxidant Capacity

Total antioxidant capacity in brain homogenate was determined by comparison with the uric acid standards using Cell Biolabs' OxiSelect™ TAC Assay (Cell Biolabs, San Diego, CA, USA, Catalog Number STA-360). The reaction was read with a standard 96-well spectrophotometric microplate reader at 490 nm (BioTek, Dubai, UAE).

2.11.4. Estimation of Lipid Peroxidation Assay: TBARS

The protocol of the OXLtek TBARS assay kit was followed for the lipid peroxidation assay (thiobarbituric acid reactive substances, ZMC catalog #0801192, Cell Biolabs, San Diego, CA, USA).

2.11.5. Histopathological Examination

For histopathological studies, the brains used were fixed for one day in a 10% formalin buffer. This was followed by washing the brains in running faucet water and then allowed to dehydrate by exposing them to serial dilutions of alcohol. Specimens were then cleaned in xylene and embedded in paraffin, carried out in an oven with hot air at 561°C for 24 h. The paraffin beeswax blocks were sectioned at 4 µm with a microtome. Glass slides were used to collect the sections of the tissues, deparaffinized, and stained with hematoxylin and eosin stains (H&E), Cresyl violet and Silver (Sigma Aldrich) following what has been reported by others [20]. Olympus light microscope (model: BX51TF, Tokyo, Japan) was utilized to examine and photograph the sections.

2.12. Statistical Analysis

The SPSS program version 16 (IBM, New York, USA) was followed. The one-way analysis of variance (ANOVA) test was employed, and the LSD-t-test was applied when equal variance could be assumed. All data was displayed as mean ± standard deviation (SD). A value of $P < 0.05$ was considered to be statistically significant.

3. RESULTS

3.1. EA-NPs' Size Determination

Average size of EA-NP was 277 nm, with PDI of 0.173. Nanoencapsulation of EA into PLGA was accomplished.

3.2. Entrapment/Loading Efficiency

EA content in the nanoparticles was estimated by comparing the absorbance at 270 nm to standard curves for different EA concentrations. The overall loading of EA in nanoparticles was found to be 0.84 w/w (84% loading). The relatively low loading efficiency is due to the presence of excessive cryoprotectant in the nanoformulations. An average of 80% loading for EA was approached in the lyophilized nanoformulation before the addition of cryoprotectant. Loading was 0.55 w/w (55% loading) after the addition of 4% mannitol as a cryoprotectant. The cryoprotectant can be removed by resuspending the nanoformulations in DI/sterile water and dialyzing it out with a 12 kDa cutoff membrane for about 3 hours (Fig. **1**).

3.3. *In vitro* Release kinetics

in vitro release kinetics of EA from EA-NP: in FBS, the immediate release of EA from EA-NP approached 25-30% after 0.5-1.0 hour, 40-50% release at 1.0-1.5 hours, followed by 50-60% sustained release at 2-6 hours and continue at 60-70% release at 9-24 hours. In contrast, no significant release was shown with PBS versus FBS.

3.4. Novel Object Recognition Test

The results of the novel recognition test are shown in (Fig. **2**), where AD group showed a significant decrease in calculated DI compared to control, EA, and EA-NP groups. Whereas AD rat models treated with EA-NP expressed a highly significant increase compared to the untreated AD group or treated with EA only (Fig. **2**).

3.5. Biomarkers for the Antioxidant Activity

The rats administered $AlCl_3$ to induce AD revealed a significant decrease in the level of catalase (109.1±5.8 ng/ml), GSH (27.1± 3.4 µM), and the total antioxidant capacity (TAC)

(530.7±3.4 CRE) in comparison to the control rat group and the rats administered EA or EA-NP. On the other hand, treatment with EA-NP enhanced the antioxidant activity and elevated levels of catalase, GSH, and TAC more than in administered EA only Table **2**.

3.6. Estimation of Lipid Peroxidation Assay: TBARS

Administration of EA-NP significantly decreased the level of TBARS to 21.3 ± 1.3 µM as compared to the high level in the case of the AD model administered $AlCl_3$ (36.5 ± 2.2 µM). The effect achieved by administration of EA-NP was lower than that of EA alone (23.8 ± 3.2 µM) Table **2**.

3.7. Histopathological Results

Sections of the cerebral cortex (CC) stained with H&E showed that groups administered EA and EA-NP did show any significant difference from control in which a normal structure was revealed (Figs. **3a**, **b**, and **c**). In the AD group, signs of degeneration were apparent: micro-vacuolation of the neuropil, condensed hyperchromatic pyknotic nuclei of neurons, vacuolation of neurons and microglia cells (Fig. **3d**). The cerebral cortex or AD rats treated with EA-NP revealed intact neurons with highly vesicular nuclei, which was improved in comparison to EA only, which still revealed some degenerated nuclei (Figs. **3e** and **f**).

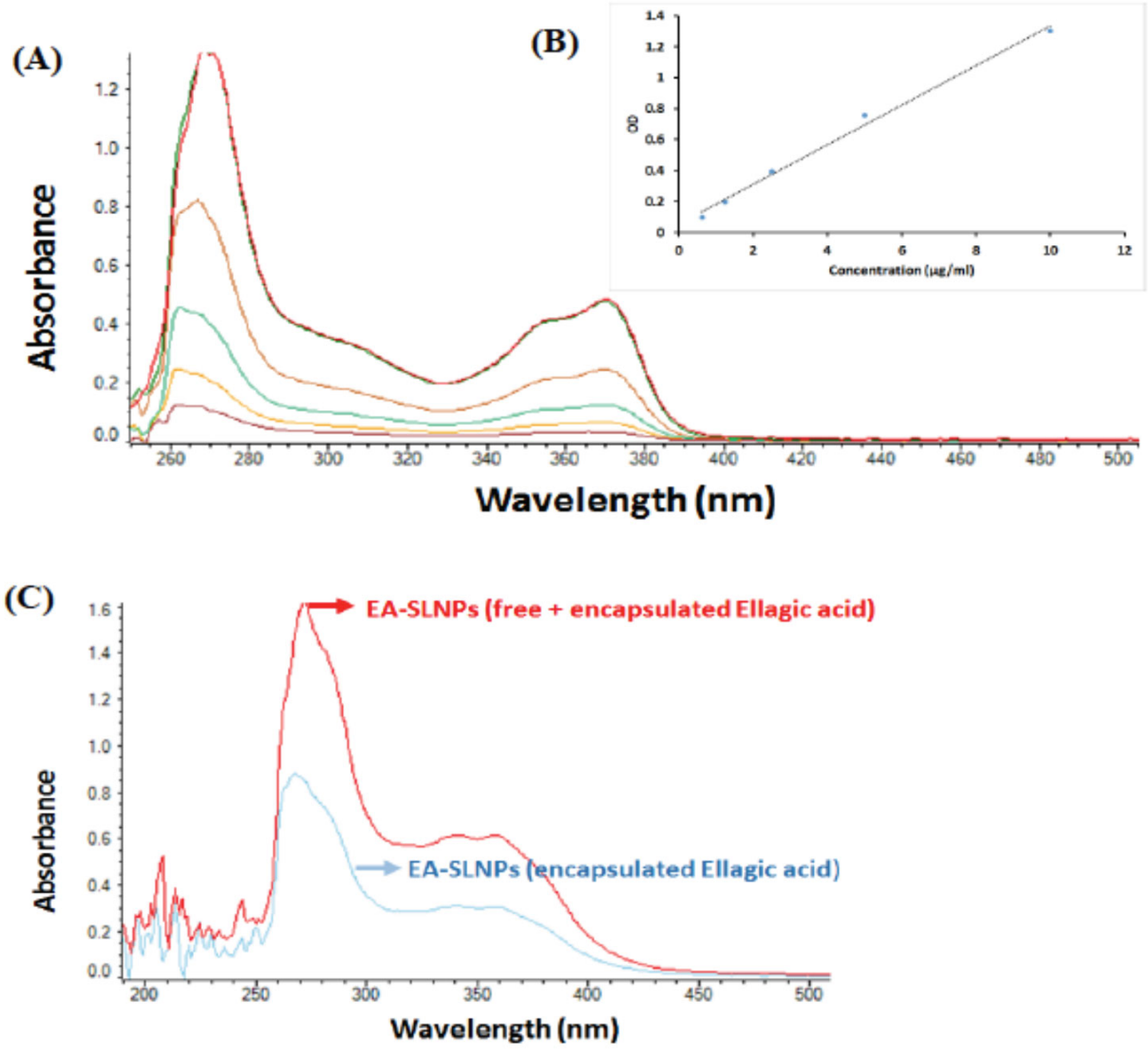

Fig. (1). Determination of entrapment/loading efficiency of EA in nanoparticles encapsulating PE (EA-NPs). (**A**) UV-VIS spectra used to construct the standard curve of EA, (**B**) with concentrations of PE of 0.625, 1.25, 2.5, 5 and 10 µg/ml, (**C**) determination of entrapment efficiency by comparing OD from UV-Vis spectra of total amount EA (free + encapsulated) and encapsulated EA in the NPs. (*A higher resolution / colour version of this figure is available in the electronic copy of the article*).

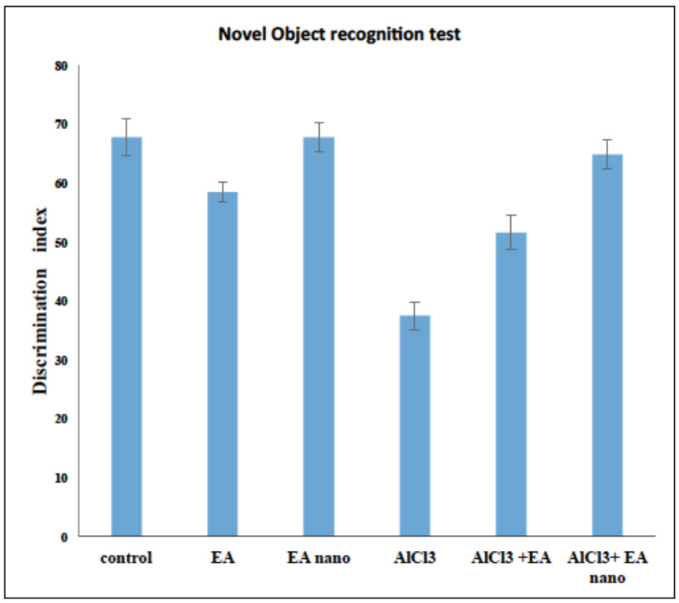

Fig. (2). Discrimination index between novel and familiar objects in all animal groups; control, treated with ellagic acid (EA), ellagic acid nanoformulation (EA-NP), AD model induced with aluminum chloride (Al Cl_3), $AlCl_3$ rats treated with EA, and $AlCl_3$ rats treated with EA-NP. Data are presented as means ± (SD).
(*) significantly different from the control, AD+EA AD+EA-NP at $P \leq 0.05$.
(**) significantly different from the AD group at $P \leq 0.05$. (*A higher resolution / colour version of this figure is available in the electronic copy of the article*).

Table 2. Catalase, glutathione activity, lipid peroxidation products (TBARS) and Total Antioxidant Capacity (TAC) in all groups.

-	Catalase ng/ml	TBARS µM	Glutathione µM	Total Antioxidant Capacity (TAC) CRE
Control	413.7 ± 3.5	20.1 ± 1.6	55 ± 3.2	891.2 ± 3.0
EA	403.1 ± 5.3	17.2 ± 1.0	54.1 ± 2.9	868.5 ± 3.4
EA-SLNP	412.4 ± 3.04	17.1 ± 2.3	57 ± 2.7	881.8 ± 4.5
AD	109.1 ± 5.8	36.5 ± 2.2	27.1 ± 3.4	530.7 ± 3.4
AD+EA	386.8 ± 3.8	23.8 ± 3.2	50.2 ± 2.5	823.4 ± 3.4
AD+EA-SLNP	423 ± 4.9	21.3 ± 1.3	58.4 ± 3.2	900.5 ± 2.5

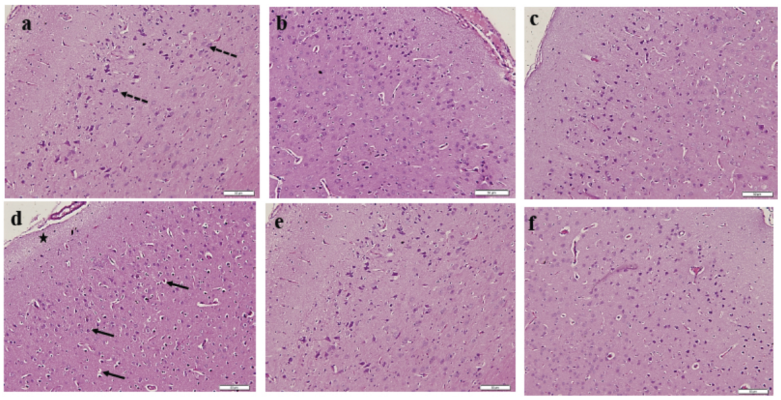

Fig. (3). Fig. **(3)**. Photomicrographs of a section of the cerebral cortex stained with H&E showing neurons of (a) control, (b) EA and (c) EA-NP having central large vesicular nuclei that contained one or more nucleoli (dashed arrows). In the Al group (d) micro-vacuolation of the neuropil (star), condensed hyperchromatic pyknotic nuclei of neurons and vacuolation of neurons (arrows). The cerebral cortex of rats treated with EA-NP (e) revealed intact neurons with highly vesicular nuclei that were more pronounced than in EA only (f). (*A higher resolution / colour version of this figure is available in the electronic copy of the article*).

Cresyl violet stain of CC of the control, EA, and EA-NP groups revealed large neurons with numerous rough endoplasmic reticulum (RER) that formed aggregates (Fig. **4a**). On the other hand, sections of AD showed central chromatolysis in which disaggregation of RER and displacement of the nucleus toward the periphery of the cell was evident (Figs. **4b**, **c**, and **d**). Nissl granules were regained upon treatment of the AD model with EA, but the effect was more pronounced with the administration of EA-NP.

Sections stained with silver revealed extracellular deposits of senile (neuritic) plaques (SP) between the neurons and neurofibrillary tangles (NFT) in the cerebral cortex of the AD model (Fig. **4d**), which were not evident in control, EA, and EA-NP groups (Figs. **5a**, **b**, **c**). Moreover, neurons of the AD model treated groups (EA-NP and EA) regained their normal structure and the SP was significantly decreased (Figs. **5e** and **f**).

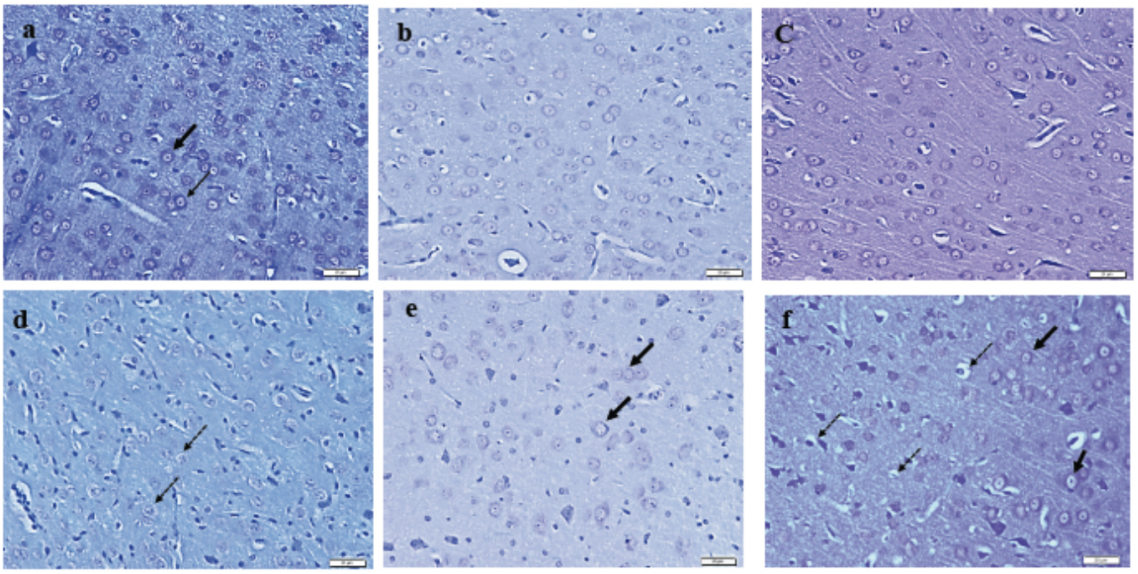

Fig. (4). Photomicrographs of a section of the cerebral cortex stained with Nissl stain showing large neurons with numerous (RER) forming the Nissl granules in the control (a), EA (b), and EA-NP (c) (dashed arrows). In the AD group (d), central chromatolysis and displacement of the nucleus toward the periphery of the cell are pointed by arrows. Nissl granules were regained upon treatment with EA-NP (e) more than in EA (f). (*A higher resolution / colour version of this figure is available in the electronic copy of the article*).

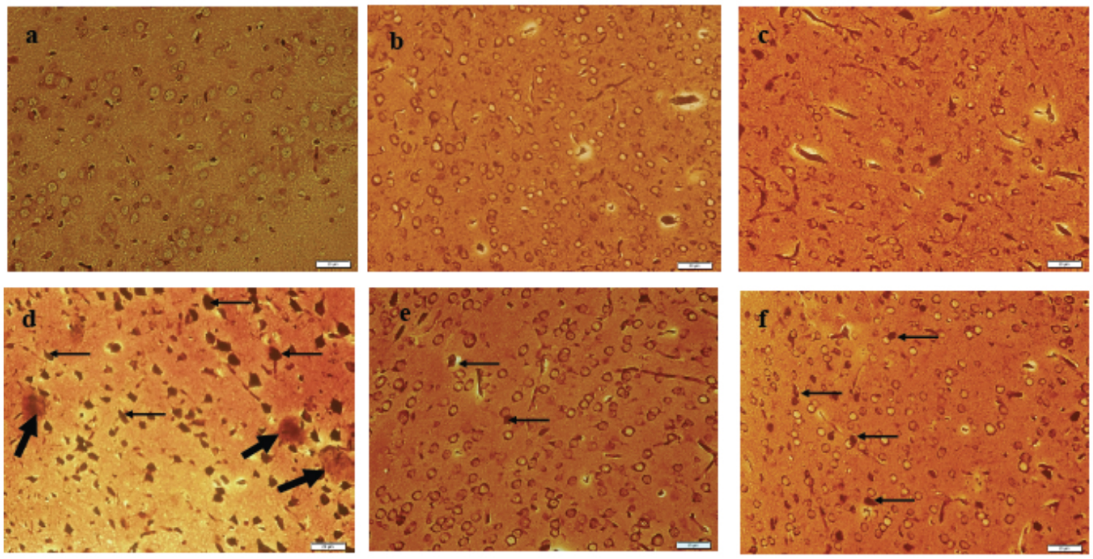

Fig. (5). Photomicrographs of a section of the cerebral cortex stained with Silver stain showing a normal structure of neurons in control (a), EA (b), and EA-NP (c) groups. In the AD group (d), extracellular deposits of senile (neuritic) plaques (SP) (thick arrows) and neurofibrillary tangles (NFT) (thin arrows) are revealed. Neurons of the EA-NP (e) and EA (f) groups regained their normal structure and the SP and NFT were significantly decreased. (*A higher resolution / colour version of this figure is available in the electronic copy of the article*).

4. DISCUSSION

AD is characterized by both progressive cognitive and behavioral impairment [21]. As cognitive function declines, psychological symptoms of dementia progressively worsen [22]. The estimated lifetime healthcare cost for a patient with AD has been estimated to be $174,000 [23]. Aluminum has been associated with cognitive impairment in mice, rabbits, and rat pups and behavioral impairment in Wistar rats [24, 25].

AD medications have not provided effective treatment yet, some research has been directed to extracts and herbs as alternative therapy for AD [26, 27]. In this regard, EA was evaluated, and two forms were used in this study.

Concerning the oral bioavailability of ellagitannins (the bioactive polyphenols in berries or pomegranate), they are not absorbed by the human gut unless hydrolyzed to EA by gastrointestinal flora [28]. Furthermore, studies showed improvement in EA pharmacokinetics with different nanoformulations, showing that increasing EA solubility is a potential approach for enhancing EA oral absorption [29].

EA is stable in the stomach and, therefore, can be a potential phytotherapeutic candidate for the development of a neuroprotective drug that can be administered orally [30]. Although there are no definitive studies to prove that EA crosses the blood-brain barrier, it was estimated that its combination with glucose would render it to cross the blood-brain barrier to induce a therapeutic effect on the central nervous system [31]. To enhance the efficacy of transport of EA to the brain, a novel EA-loaded nanoparticles formulation was used in the present study with the hypothesis that it offers a better therapeutic potential.

Studies have indicated that the brain is subjected to free radical induced lipid peroxidation because it uses around one-third of the inspired oxygen and as such exposes the lipids and proteins, which represent the major structural and functional components of the cell membrane, to oxidative stress and results in neurodegenerative disorders [32, 33].

In this study, it was determined that levels of catalase, GSH, and the TAC were all decreased in the homogenate of brains of AD rat models resulting in antioxidant enzyme dysfunction. However, lipid peroxidation (TBRAS) level was increased. This was associated with marked histopathological changes manifested as neuronal swelling, signs of chromatolysis, vacuolation, and pyknotic changes of the neurons. This was in addition to the characteristic degenerative signs of AD; amyloid beta peptide plaques and neurofibrillary tangles. This was reflected in the animal cognition, where the calculated DI was the lowest in the case of AD animals.

This is supported by Paschen, W. and Mengesdorf, T. (2005) [34] who reported that although the mechanism underlying Nissl substance changes remains unclear, malfunction of the rough endoplasmic reticulum (RER) and stress, which forms part of the Nissl substance, can result in neurodegenerative disorders.

H_2O_2 is considered the most toxic molecule to the brain. The neuronal defense against it is mediated primarily by the GSH system. The increase in lipid peroxidation may be due to depletion of GSH content in the brain [35]. Moreover, the gradual buildup of advanced glycation end products in body tissues is considered a major contributor to AD because it could bind to receptors (RAGE) on the surface of the cell, activate cell signaling, and lead to the production of reactive oxygen species and inflammatory factors. Consequently, proteins on the extracellular matrix crosslink with other matrix components, leading to a loss in their function [36]. Habib *et al*. (2010) reported that amyloid-beta specifically bound purified catalase with high affinity and inhibited catalase breakdown of H_2O_2 [37]. The amyloid-beta-induced catalase inhibition was involved in the formation of the inactive catalase Compound II.

The present results are in accordance with those of Cristalli *et al*. (2012), who stated that the lipid peroxidation products (T-BRAS) level increased with the severity of cognitive dysfunction in AD [38]. Similarly, it has been shown that the increase of peroxidation in the brains of AD cases was related to increased levels of beta peptide [39].

Here, it was also observed that simultaneous administration of EA-NP with $AlCl_3$ increased the levels of catalase, GSH and TAC in brain homogenate more than when administered with EA only. This increase was reflected on decrease in the level of TBARS and in the amyloid-beta peptide plaques and neurofibrillary tangles in silver stained sections. It is documented that EA inhibits β-secretase activity and thus holding neurotoxicity [40]. It also has antioxidant and anti-inflammatory properties that enhance learning and memory deficits in the AD rat model [41]. Improvement in cognitive function was also reported in a previous research where levels of the DI increased in groups treated with EA in comparison to the AD rat model [42].

It appears that the nanoformulation was better at crossing the blood-brain barrier (BBB) and delivering the greater antioxidant activities of EA to the brain, which would be expanded in our future studies to determine the BBB permeability of EA for EA versus Nano-EA. This is supported by Kreuter (2004), who noted that polysorbate (Tween) coated nanoparticles resulted in enhanced transport of drugs across the blood-brain barrier by endocytosis *via* the low-density lipoprotein (LDL) receptor of the endothelial cells as a consequence of adsorption of lipoproteins form blood plasma to the nanoparticles [43]. It was postulated that the recognition and interaction with lipoprotein receptors on brain capillary endothelial cells are likely to be the reason behind the brain uptake of the drug [44].

LIMITATIONS AND FUTURE STUDIES

The potential protective efficacy of EA-SLNP versus EA against AlCl3 - induced brain AD oxidative reactivity, impaired neuronal and cognitive functions, which indicates that EA-SLNP was better at crossing the blood-brain barrier (BBB) and delivering the powerful antioxidant EA to the brain. Yet, a limitation of this study is the absence of other techniques that explains the uptake across the BBB. Hence, future studies will focus on examining the pharmacokinetics (EA blood levels over time) and the BBB of EA (EA levels in brain areas over time) with EA nanoformulations versus EA.

CONCLUSION

EA nanoformulation treatment was more effective than EA alone treatment and counteracted the reactive oxidant activity of $AlCl_3$ in the cerebral cortex of rats inducing AD, enhanced cognitive function, and repaired structural pathological changes.

ETHICS APPROVAL AND CONSENT TO PARTICIPATE

Ethical approval for the study was granted from the Ethical Review Committee of King Abdulaziz University. (Reference No. 328-19) Animal study.

HUMAN AND ANIMAL RIGHTS

The protocol of the current study was in accordance with the guidelines set by the animal care facility at KAU following all regu-

lations issued by "The National Committee of Bio and Medical Ethics- King Abdulaziz City for Science and Technology".

CONSENT FOR PUBLICATION

Not applicable.

AVAILABILITY OF DATA AND MATERIALS

Not applicable.

FUNDING

This project was funded by the Deanship of Scientific Research (DSR) at King Abdulaziz University, Jeddah, under grant no. G: 1574-140-1440.

CONFLICT OF INTEREST

The authors have no conflicts of interest, financial or otherwise.

ACKNOWLEDGEMENTS

The authors acknowledge with thanks The DSR for technical and financial support.

REFERENCES

[1] Anand, R.; Gill, K. D.; Mahdi, A. A. Therapeutics of Alzheimer's disease: Past, present and future. *Neuropharmacology,* **2014**, *76*(4), 27-50.

[2] Tosato, M.; Zamboni, V.; Ferrini, A.; Cesari, M. The aging process and potential interventions to extend life expectancy. *Clin. Interv. Aging,* **2007**, *2*(3), 401-412. PMID: 18044191

[3] Mangialasche, F.; Polidori, M.C.; Monastero, R.; Ercolani, S.; Camarda, C.; Cecchetti, R.; Mecocci, P. Biomarkers of oxidative and nitrosative damage in Alzheimer's disease and mild cognitive impairment. *Ageing Res. Rev.,* **2009**, *8*(4), 285-305. http://dx.doi.org/10.1016/j.arr.2009.04.002 PMID: 19376275

[4] Mohsenzadegan, M.; Mirshafiey, A. The immunopathogenic role of reactive oxygen species in Alzheimer disease. *Iran. J. Allergy Asthma Immunol.,* **2012**, *11*(3), 203-216. PMID: 22947905

[5] Özkaya, A. Adıyaman Univ., Faculty of Science, Adıyaman (Turkey). Div. of Chemistry; Çelik, S., Bingöl Univ., Faculty of Science, Bingöl (Turkey). Div. of Chemistry; Yüce, A., Fırat University, Faculty of Veterinary Medicine, Elazığ (Turkey). Div. of Physiology; Şahin, Z., Bitlis Eren Univ., Vocational School of Health, Bitlis (Turkey); Yılmaz, Ö., Fırat University, Faculty of Science, Elazığ (Turkey). Div. of Biology, The effects of ellagic acid on some biochemical parameters in the liver of rats against oxidative stress induced by aluminum. *Journal of the Faculty of Veterinary Medicine, University of Kafkas, Kars (Turkey),* **2018**, , 263-268.

[6] Rosillo, M.A.; Sánchez-Hidalgo, M.; Cárdeno, A.; Aparicio-Soto, M.; Sánchez-Fidalgo, S.; Villegas, I.; de la Lastra, C.A. Dietary supplementation of an ellagic acid-enriched pomegranate extract attenuates chronic colonic inflammation in rats. *Pharmacol. Res.,* **2012**, *66*(3), 235-242. http://dx.doi.org/10.1016/j.phrs.2012.05.006 PMID: 22677088

[7] Malik, A.; Afaq, S.; Shahid, M.; Akhtar, K.; Assiri, A. Influence of ellagic acid on prostate cancer cell proliferation: a caspase-dependent pathway. *Asian Pac. J. Trop. Med.,* **2011**, *4*(7), 550-555. http://dx.doi.org/10.1016/S1995-7645(11)60144-2 PMID: 21803307

[8] Palinisamy, M.G.K.; Murugan, R. Antidiabetic efficacy of ellagic acid in streptozotocin induced diabetes mellitus in albino wistar rats. *Asian J Pharm Clin Res,* **2011**, *4*, 124-128.

[9] Rani, U.P.; Kesavan, R.; Ganugula, R.; Avaneesh, T.; Kumar, U.P.; Reddy, G.B.; Dixit, M. Ellagic acid inhibits PDGF-BB-induced vascular smooth muscle cell proliferation and prevents atheroma formation in streptozotocin-induced diabetic rats. *J. Nutr. Biochem.,* **2013**, *24*(11), 1830-1839. http://dx.doi.org/10.1016/j.jnutbio.2013.04.004 PMID: 23866995

[10] Hamad, A-W.R.; Al-Momani, W.M.; Janakat, S.; Oran, S.A. Bioavailability of Ellagic Acid After Single Dose Administration Using HPLC. *Pak. J. Nutr.,* **2009**, *8*(10), 1661-1664. http://dx.doi.org/10.3923/pjn.2009.1661.1664

[11] Lee, R.W.; Shenoy, D.B.; Sheel, R. CHAPTER 2 - Micellar Nanoparticles: Applications for Topical and Passive Transdermal Drug Delivery.*Handbook of Non-Invasive Drug Delivery Systems*; Kulkarni, V.S., Ed.; William Andrew Publishing: Boston, **2010**, pp. 37-58. http://dx.doi.org/10.1016/B978-0-8155-2025-2.10002-2

[12] Shirode, A.B.; Bharali, D.J.; Nallanthighal, S.; Coon, J.K.; Mousa, S.A.; Reliene, R. Nanoencapsulation of pomegranate bioactive compounds for breast cancer chemoprevention. *Int. J. Nanomedicine,* **2015**, *10*, 475-484. PMID: 25624761

[13] Kuo, Y.C.; Chung, J.F. Physicochemical properties of nevirapine-loaded solid lipid nanoparticles and nanostructured lipid carriers. *Colloids Surf. B Biointerfaces,* **2011**, *83*(2), 299-306. http://dx.doi.org/10.1016/j.colsurfb.2010.11.037 PMID: 21194902

[14] Quafa, R. N. E., Chronic Exposure to Aluminum Chloride in Mice: Exploratory Behaviors and Spatial Learning - Semantic Scholar. *Adv. Biol. Res. (Faisalabad),* **2008**, *2*(1-2), 26-33.

[15] Antunes, M.; Biala, G. The novel object recognition memory: neurobiology, test procedure, and its modifications. *Cogn. Process.,* **2012**, *13*(2), 93-110. http://dx.doi.org/10.1007/s10339-011-0430-z PMID: 22160349

[16] Grayson, B.; Idris, N.F.; Neill, J.C. Atypical antipsychotics attenuate a sub--chronic PCP-induced cognitive deficit in the novel object recognition task in the rat. *Behav. Brain Res.,* **2007**, *184*(1), 31-38. http://dx.doi.org/10.1016/j.bbr.2007.06.012 PMID: 17675172

[17] Kumar, P.; Kumar, A. Neuroprotective effect of cyclosporine and FK506 against 3-nitropropionic acid induced cognitive dysfunction and glutathione redox in rat: possible role of nitric oxide. *Neurosci. Res.,* **2009**, *63*(4), 302-314. http://dx.doi.org/10.1016/j.neures.2009.01.005 PMID: 19367792

[18] Aebi, H. *C., Methods in enzymatic analysis*; Acadamic press: New York, **1974**, Vol. 2, .

[19] Ellman, G.L. Tissue sulfhydryl groups. *Arch. Biochem. Biophys.,* **1959**, *82*(1), 70-77. http://dx.doi.org/10.1016/0003-9861(59)90090-6 PMID: 13650640

[20] Bancroft, J.D.S.A. The haematoxylin and eosin.*Theory and Practice of Histological Techniques,* 4th ed; Livingstone, C., Ed.; London, New York, Tokyo, **1996**, pp. 99-113.

[21] Robert, P. H.; Verhey, F. R.; Byrne, E. J.; Hurt, C.; De Deyn, P. P.; Nobili, F.; Riello, R.; Rodriguez, G.; Frisoni, G. B.; Tsolaki, M.; Kyriazopoulou, N.; Bullock, R.; Burns, A.; Vellas, B. Grouping for behavioral and psychological symptoms in dementia: clinical and biological aspects. *Consensus paper of the European Alzheimer disease consortium. European psychiatry : the journal of the Association of European Psychiatrists,* **2005**, *20*(7), 490-6.

[22] Aalten, P.; Jolles, J.; de Vugt, M.E.; Verhey, F.R. The influence of neuropsychological functioning on neuropsychiatric problems in dementia. *J. Neuropsychiatry Clin. Neurosci.,* **2007**, *19*(1), 50-56. http://dx.doi.org/10.1176/jnp.2007.19.1.50 PMID: 17308227

[23] Zhu, C.W.; Sano, M. Economic considerations in the management of Alzheimer's disease. *Clin. Interv. Aging,* **2006**, *1*(2), 143-154. http://dx.doi.org/10.2147/ciia.2006.1.2.143 PMID: 18044111

[24] Golub, M.S.; Germann, S.L. Long-term consequences of developmental exposure to aluminum in a suboptimal diet for growth and behavior of Swiss Webster mice. *Neurotoxicol. Teratol.,* **2001**, *23*(4), 365-372. http://dx.doi.org/10.1016/S0892-0362(01)00144-1 PMID: 11485839

[25] Buraimoh, A.A.; Ojo, S.A.; Hambolu, J.O.; Adebisi, S.S. Behavioural Enpoints of Adult Wistar Rats, Following Aluminium Chloride Exposure. *Br. J. Pharmacol. Toxicol.,* **2011**, *2*(5), 273-276.

[26] Akhondzadeh, S.; Abbasi, S.H. Herbal medicine in the treatment of Alzheimer's disease. *Am. J. Alzheimers Dis. Other Demen.,* **2006**, *21*(2), 113-118. http://dx.doi.org/10.1177/153331750602100211 PMID: 16634467

[27] Downey, L.A.; Kean, J.; Nemeh, F.; Lau, A.; Poll, A.; Gregory, R.; Murray, M.; Rourke, J.; Patak, B.; Pase, M.P.; Zangara, A.; Lomas, J.; Scholey, A.; Stough, C. An acute, double-blind, placebo-controlled crossover study of 320 mg and 640 mg doses of a special extract of Bacopa monnieri (CDRI 08) on sustained cognitive performance. *Phytother. Res.,* **2013**, *27*(9), 1407-1413. http://dx.doi.org/10.1002/ptr.4864 PMID: 23281132

[28] Larrosa, M.; Tomás-Barberán, F.A.; Espín, J.C. The dietary hydrolysable tannin punicalagin releases ellagic acid that induces apoptosis in human colon adenocarcinoma Caco-2 cells by using the mitochondrial pathway. *J. Nutr. Biochem.,* **2006**, *17*(9), 611-625. http://dx.doi.org/10.1016/j.jnutbio.2005.09.004 PMID: 16426830

[29] Ceci, C.; Graziani, G.; Faraoni, I.; Cacciotti, I. Strategies to improve ellagic acid bioavailability: from natural or semisynthetic derivatives to nanotechnological approaches based on innovative carriers. *Nanotechnology,* **2020**, *31*(38), 382001. http://dx.doi.org/10.1088/1361-6528/ab912c PMID: 32380485

[30] Usta, C.; Ozdemir, S.; Schiariti, M.; Puddu, P.E. The pharmacological use of ellagic acid-rich pomegranate fruit. *Int. J. Food Sci. Nutr.,* **2013**, *64*(7), 907-913. http://dx.doi.org/10.3109/09637486.2013.798268 PMID: 23700985

[31] Kyriakis, E.; Stravodimos, G.A.; Kantsadi, A.L.; Chatzileontiadou, D.S.; Skamnaki, V.T.; Leonidas, D.D. Natural flavonoids as antidiabetic agents. The binding of gallic and ellagic acids to glycogen phosphorylase b. *FEBS Lett.,* **2015**, *589*(15), 1787-1794. http://dx.doi.org/10.1016/j.febslet.2015.05.013 PMID: 25980608

[32] Gella, A.; Durany, N. Oxidative stress in Alzheimer disease. *Cell Adhes. Mi-*

gr., **2009**, *3*(1), 88-93.
http://dx.doi.org/10.4161/cam.3.1.7402 PMID: 19372765
[33] Lobo, V.; Patil, A.; Phatak, A.; Chandra, N. Free radicals, antioxidants and functional foods: Impact on human health. *Pharmacogn. Rev.,* **2010**, *4*(8), 118-126.
http://dx.doi.org/10.4103/0973-7847.70902 PMID: 22228951
[34] Paschen, W.; Mengesdorf, T. Endoplasmic reticulum stress response and neurodegeneration. *Cell Calcium,* **2005**, *38*(3-4), 409-415.
http://dx.doi.org/10.1016/j.ceca.2005.06.019 PMID: 16087231
[35] Schuessel, K.; Leutner, S.; Cairns, N.J.; Müller, W.E.; Eckert, A. Impact of gender on upregulation of antioxidant defence mechanisms in Alzheimer's disease brain. *J. Neural Transm. (Vienna),* **2004**, *111*(9), 1167-1182.
http://dx.doi.org/10.1007/s00702-004-0156-5 PMID: 15338332
[36] Srikanth, V.; Maczurek, A.; Phan, T.; Steele, M.; Westcott, B.; Juskiw, D.; Münch, G. Advanced glycation endproducts and their receptor RAGE in Alzheimer's disease. *Neurobiol. Aging,* **2011**, *32*(5), 763-777.
http://dx.doi.org/10.1016/j.neurobiolaging.2009.04.016 PMID: 19464758
[37] Habib, L.K.; Lee, M.T.; Yang, J. Inhibitors of catalase-amyloid interactions protect cells from beta-amyloid-induced oxidative stress and toxicity. *J. Biol. Chem.,* **2010**, *285*(50), 38933-38943.
http://dx.doi.org/10.1074/jbc.M110.132860 PMID: 20923778
[38] Cristalli, D.O.; Arnal, N.; Marra, F.A.; de Alaniz, M.J.; Marra, C.A. Peripheral markers in neurodegenerative patients and their first-degree relatives. *J. Neurol. Sci.,* **2012**, *314*(1-2), 48-56.
http://dx.doi.org/10.1016/j.jns.2011.11.001 PMID: 22113180
[39] Butterfield, D.A.; Castegna, A.; Lauderback, C.M.; Drake, J. Evidence that amyloid beta-peptide-induced lipid peroxidation and its sequelae in Alzheimer's disease brain contribute to neuronal death. *Neurobiol. Aging,* **2002**, *23*(5), 655-664.
http://dx.doi.org/10.1016/S0197-4580(01)00340-2 PMID: 12392766
[40] Kwak, H.M.; Jeon, S.Y.; Sohng, B.H.; Kim, J.G.; Lee, J.M.; Lee, K.B.; Jeong, H.H.; Hur, J.M.; Kang, Y.H.; Song, K.S. beta-Secretase (BACE1) inhibitors from pomegranate (Punica granatum) husk. *Arch. Pharm. Res.,* **2005**, *28*(12), 1328-1332.
http://dx.doi.org/10.1007/BF02977896 PMID: 16392663
[41] Kiasalari, Z.; Heydarifard, R.; Khalili, M.; Afshin-Majd, S.; Baluchnejadmojarad, T.; Zahedi, E.; Sanaierad, A.; Roghani, M. Ellagic acid ameliorates learning and memory deficits in a rat model of Alzheimer's disease: an exploration of underlying mechanisms. *Psychopharmacology (Berl.),* **2017**, *234*(12), 1841-1852.
http://dx.doi.org/10.1007/s00213-017-4589-6 PMID: 28303372
[42] Braidy, N.; Selvaraju, S.; Essa, M.M.; Vaishnav, R.; Al-Adawi, S.; Al-Asmi, A.; Al-Senawi, H.; Abd Alrahman Alobaidy, A.; Lakhtakia, R.; Guillemin, G.J. Neuroprotective effects of a variety of pomegranate juice extracts against MPTP-induced cytotoxicity and oxidative stress in human primary neurons. *Oxid. Med. Cell. Longev.,* **2013**, *2013*, 685909.
http://dx.doi.org/10.1155/2013/685909 PMID: 24223235
[43] Kreuter, J. Influence of the surface properties on nanoparticle-mediated transport of drugs to the brain. *J. Nanosci. Nanotechnol.,* **2004**, *4*(5), 484-488.
http://dx.doi.org/10.1166/jnn.2003.077 PMID: 15503433
[44] Michaelis, K.; Hoffmann, M.M.; Dreis, S.; Herbert, E.; Alyautdin, R.N.; Michaelis, M.; Kreuter, J.; Langer, K. Covalent linkage of apolipoprotein e to albumin nanoparticles strongly enhances drug transport into the brain. *J. Pharmacol. Exp. Ther.,* **2006**, *317*(3), 1246-1253.
http://dx.doi.org/10.1124/jpet.105.097139 PMID: 16554356